Nuclear Mathematical and Computational Sciences: A Century in Review, A Century Anew
Gatlinburg, Tennessee, April 6-11, 2003, on CD-ROM, American Nuclear Society, LaGrange Park, IL (2003)

DEPENDENCE OF BRACHYTHERAPY DOSIMETRY ON THE UNIFORMITY OF THE ISOTOPE PHYSICAL DISTRIBUTION

Mark J. Rivard
Department of Radiation Oncology, Tufts - New England Medical Center
750 Washington Street, Box #246
Boston, MA 02111, USA
mrivard@lifespan.org

Bernadette L. Kirk and Luiz C. Leal
Nuclear Data and Information Analysis Group, Nuclear Science and Technology Division
Oak Ridge National Laboratory
Oak Ridge, TN 37831, USA
blk@ornl.gov; e5a@ornl.gov

ABSTRACT

The MCNP radiation transport code was used to assess the impact of non-uniform ^{125}I distribution within a clinical brachytherapy source containing four ion exchange resin beads. Results from a previous study using uniform ^{125}I distributions and modified photon cross-section libraries were compared to those obtained using non-uniform distributions and the same modified cross-section libraries. Uniformity was varied by selecting to activate only certain resin beads within the capsule. Changes in the resulting dose rate distribution were expressed in terms of the American Association of Physicists in Medicine (AAPM) Task Group No. 43 Report brachytherapy dosimetry formalism. Upon varying the ^{125}I physical distribution, while retaining the same overall radioactivity, the dose rate distribution along the capsule transverse-plane remained constant within 5% for $r > 0.5$ cm. For $r \leq 0.5$ cm, the geometric effects of the resin beads dominated the intrasource shielding effects, and dose rate distributions varied by as much as a factor of 3 at $r = 0.05$ cm for the second most superiorly positioned resin bead. For points off the transverse-plane, comparisons of the uniform and non-uniform dose rate distributions produced larger variations. At $r = 0.25$, 1, and 5 cm, dose rate distributions varied by a factor of 2.4, 1.7, and 1.4 along the superior direction of the source long-axis, and variations by a factor of 3.0, 1.8, and 1.4 were observed along the inferior direction, respectively. Since intrasource shielding effects were virtually constant along the source long-axes, these results justify the finding that anisotropy variations were largely dependent on geometric effects.

Key Words: MCNP, brachytherapy, radiation dosimetry, TG-43

1. INTRODUCTION

Monte Carlo radiation transport techniques have been used for over three decades to characterize brachytherapy source dosimetry [1]. ^{125}I sources have been in clinical use for approximately the same time period, but new source models have been introduced into market over the past five years. Consequently, the American Association of Physicists in Medicine (AAPM) requires publication of requisite dosimetry data preceding clinical implementation [2]. This requisite

dosimetry data is a consensus of results from experiments and from Monte Carlo methods for use in the AAPM Task Group No. 43 Report (TG-43) brachytherapy dosimetry formalism [3,4]. In addition to providing the requisite dosimetry data required for clinical implementation of new brachytherapy sources [5,6], our group has investigated the merits of realistic modeling and parametric analysis of dosimetry parameter dependence [7-9].

In this study, we extend this research to determine the dependence of ^{125}I distribution uniformity within a clinical brachytherapy source. While brachytherapy sources are generally expected to be uniformly loaded, it is of interest to examine the limitations of this assumption and to determine the clinical significance of the non-uniformity.

2. MATERIALS & METHODS

2.1. ^{125}I Brachytherapy Source

The type of ^{125}I brachytherapy source examined in this study is comprised of a titanium capsule containing two gold-copper radio-opaque markers (used for source localization) and four ion exchange resin beads containing the ^{125}I. The geometry and construction of this source type has been previously well-documented [7,10], but a diagram of the source is depicted in Fig.1 for reader convenience. Starting from the top (superior) sphere within the capsule, the internal components are: resin bead #1, resin bead #2, marker #1, marker #2, resin bead #3, and resin bead #4. The (x,y,z) coordinates for beads #1 through #4 are (0,-0.01,0.064), (0,-0.01,0.014), (0,-0.01,-0.136), and (0,0,-0.185), respectively. Coordinate system origin is denoted by the + symbol located within resin bead #2.

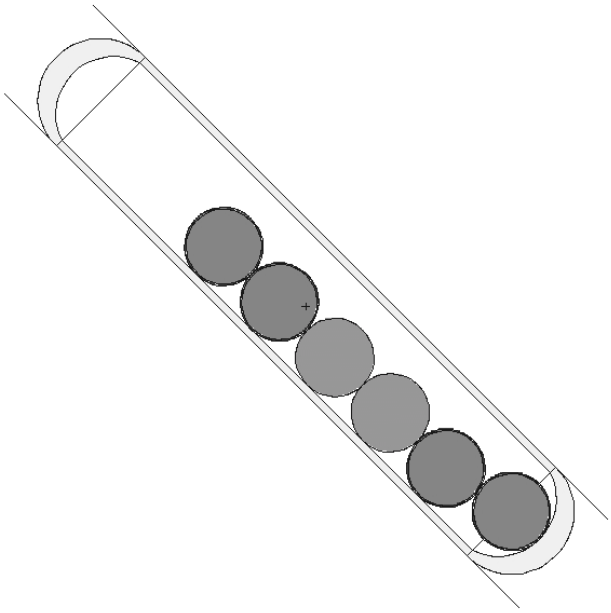

Figure 1. Diagram of the ^{125}I brachytherapy source illustrating the internal components (four resin beads and two radiographic markers).

2.2. Variations in ^{125}I Uniformity

Historically, brachytherapy dosimetry using Monte Carlo methods assumes a uniform distribution of the radioisotope. For the ^{125}I source type examined herein, the total amount of radioisotope would be uniformly distributed among the four resin beads. Dosimetry results based on this assumption were previously obtained according to TG-43 dosimetry formalism in a 30 cm diameter liquid water phantom using a polar coordinate system with 0.1 cm and 1º radial and angular resolution, respectively [10].

For the current study, the dosimetric impact of each of the four radioactive resin beads was assessed by modeling circumstances where only one resin bead was laden with radioactive ^{125}I and the remaining three were non-radioactive. Consequently, four different Monte Carlo studies were performed. The first study modeled resin bead #1 with radioactive ^{125}I with the remaining resin beads made non-radioactive. The second study modeled bead #2 with radioactive ^{125}I with the remaining beads made non-radioactive, and so on. These results were compared with results from the previously performed Monte Carlo studies assuming uniform ^{125}I distribution among the four resin beads [10]. Impact on the dose rate distribution both relative and absolute dosimetry parameters was quantified as a function of radial distance from and polar angle about the ^{125}I brachytherapy source. To demonstrate validity of the superposition-method presumption upon which this study was largely-based, a final Monte Carlo study modeled equal radioactivity in beads #1 and #3 for comparison with the equally-weighted results from the bead #1 and bead #3 Monte Carlo studies. Expressed symbolically, this study aimed to determine if (1)+(3) = (1+3), and was performed to test the assumption that: (1)+(2)+(3)+(4) = (1+2+3+4) with (1+2+3+4) data taken from reference 10.

2.3. Computer Platform Used to Estimate Dose Distributions

To perform radiation transport calculations in a timely manner, we employed the use of the CPile Linux Cluster at Oak Ridge National Laboratory [11]. The MCNP 4C software was installed [12], and the DLC-200 photon cross-section libraries for elements H, C, N, O, Ar, and Ti were replaced with customized cross-sections based on more recent XCOM data [10,13,14]. For comparison, runs were also performed using MCNP4B2 on a parallel system of PCs [15,16], and no statistically significant differences were observed between the two systems for nps $\geq 10^9$ histories; thus demonstrating the equivalence of MCNP4B2 and MCNP4C for this application.

3. RESULTS & DISCUSSION

3.1. Comparison of Transverse-Plane Dose Distributions

Compared to their combined contributions, the relative contributions from each of the four resin beads are plotted in Fig. 2. Here it is evident that the four beads have approximately equal dose contribution to the transverse-plane dose at radial distances beyond 1 cm. For these locations, the relative dose contributions from resin beads #1 through #4 were 25.8%, 25.1%, 25.1%, and 24.0%, respectively. For $r \leq 0.5$ cm, the dose contributions from resin bead #2 escalates. This behavior is likely due to geometric effect of increasing proximity to bead #2 as compared to distances from other beads. Also for $r \leq 0.5$ cm, contributions from resin beads #3 and #4

diminish. Because the radio-opaque markers block ^{125}I radiation, this decrease is likely due to a combination of geometric effects and marker shielding. The relative dose contribution from resin bead #1 exhibits peculiar behavior. Dose contribution increases for $0.1 < r < 0.5$ cm, and decreases for $r < 0.1$ cm. As expected, the increase is attributed to decreasing proximity while the decrease is resin bead #2 blocking the ^{125}I radiation from resin bead #1. For all resin beads, data were unavailable for $r < 0.05$ cm due to positioning within the source encapsulation.

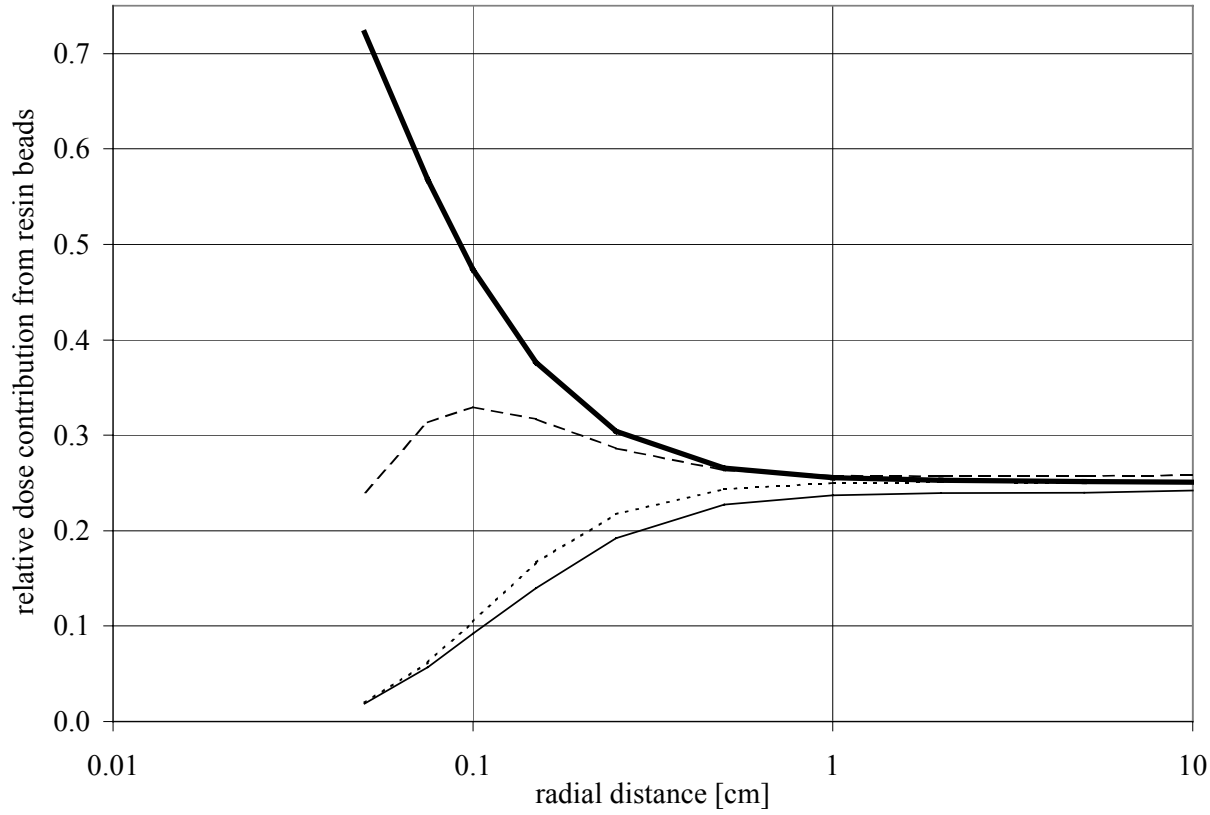

Figure 2. Relative dose contributions from the four ^{125}I resin beads as a function of radial distance. Starting from the uppermost curve, the bold, dashed, dotted, and line curves represent contributions from resin beads #2, #1, #3, and #4, respectively.

3.2. Comparison of Dose Distributions Off the Transverse-Plane

The dose distributions off the transverse-plane are typically normalized to the transverse-plane ($\theta = 90^{o}$) data and referred to as 2-D anisotropy functions [4,17]. The 2-D anisotropy functions for the four resin bead combination are presented in Fig. 3 [10]. For small distances (e.g., 0.25 cm, it was hypothesized that dose contributions from resin beads #1 and #4 would dominate the combined dose distribution as the polar angle θ approaches 0^{o} and 180^{o}, respectively. This was thought due to increased proximity to the point in question, and due to shielding of the other three resin beads.

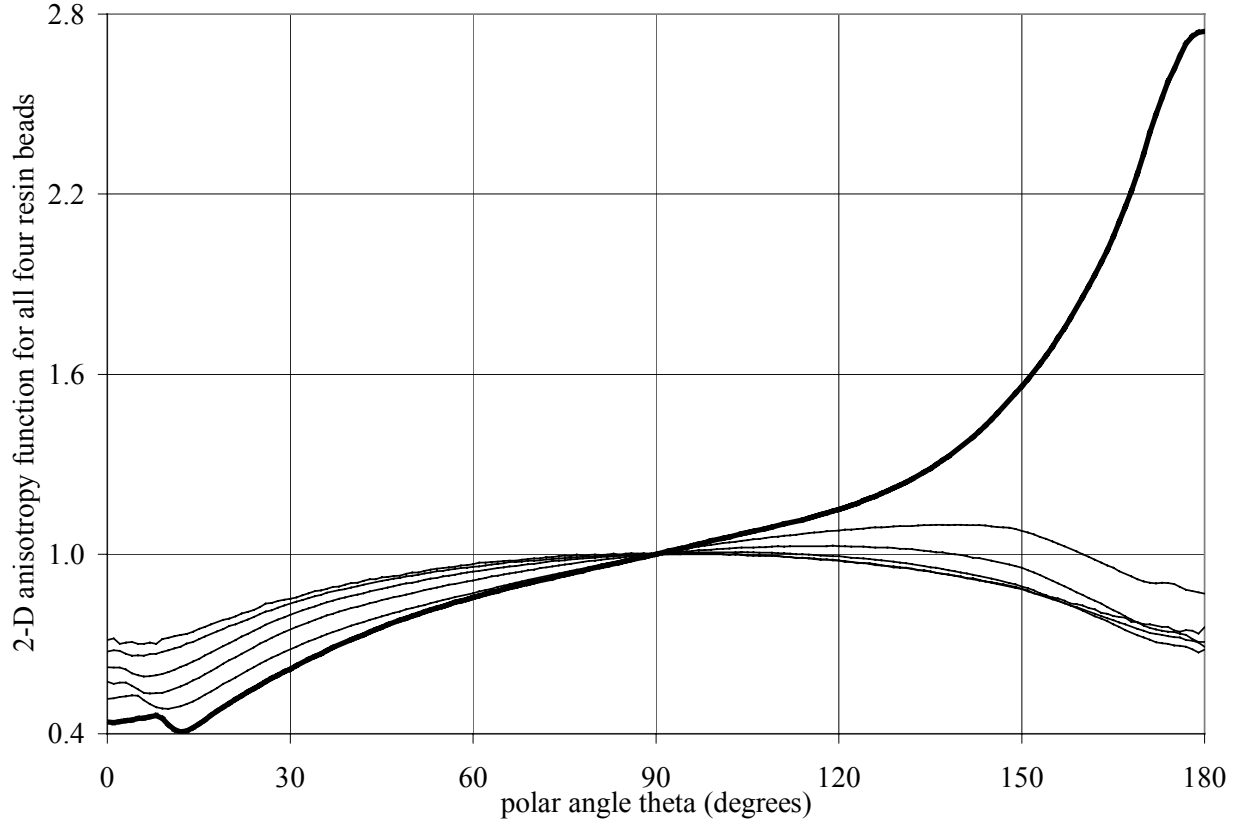

Figure 3. The bolded curve depicts the r = 0.25 cm data. For θ < 90º, the r = 0.5, 1, 2, 5, and 10 cm data proceed sequentially above the r = 0.25 cm curve. The slight undulation at 5º < θ < 15º is due to variable attenuation by the superior end weld of the titanium encapsulation.

Contributions to the combined 2-D anisotropy dose distributions from each of the four resin beads at various distances is depicted in Fig. 4a through 4d for beads #1 through #4, respectively.

Fig. 5a through Fig. 5f compare the resin bead contributions to the 2-D anisotropy function at distances of 0.25, 0.5, 1, 2, 5, and 10 cm, respectively. Resin beads #1 and #4 are indicated by bold lines, and are highest at θ = 0º and 180º, respectively. Resin beads #2 and #3 are indicated by normal curves, and are also highest at θ = 0º and 180º, respectively. For the r = 0.25 cm data, it is evident that the θ = 0º and θ = 180º 2-D anisotropy data are largely determined by the activities of resin beads #1 and #4, respectively. As radial distance increases towards 10 cm, the contributions from resin bead #3 approach that delivered by resin bead #4. However, contributions from resin bead #2 do not equally approach those delivered by resin bead #1. This difference in contributions is thought due to the intrasource shielding caused by bead-specific geometries where resin beads #1 and #2 share the same x- and y-axis coordinates while there is a

slight y-axis offset between resin beads #3 and #4 which comparatively minimizes shielding of bead #3 by bead #4.

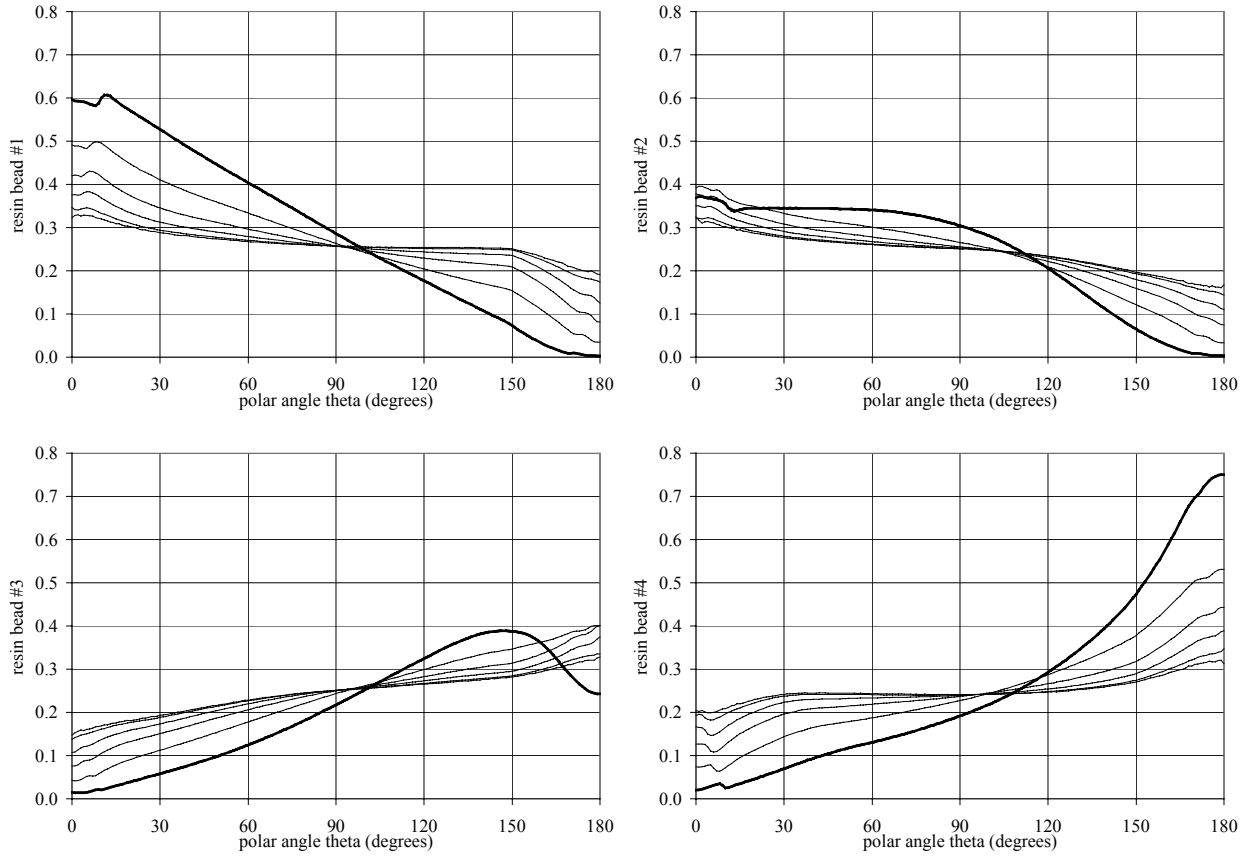

Figure 4. Contributions to the 2-D anisotropy function from each of the four resin beads. Fig. 4a through Fig. 4d depict the contributions from resin beads #1 through #4, respectively. The bolded curve is the r = 0.25 cm data, and the r = 0.5, 1, 2, 5, and 10 cm data proceed sequentially above the r = 0.25 cm curve. To readily permit comparisons, the ordinate scale did not vary among the four graphs. Undulations at $5^{o} < \theta < 15^{o}$ and $165^{o} < \theta < 175^{o}$ are due to variable attenuation by the superior and inferior end welds of the titanium encapsulation, respectively.

At r = 0.25, 1, and 5 cm, dose rate distributions varied from the nominal 25% contribution by a factor of 2.4, 1.7, and 1.4 along the superior direction of the source long-axis (caused by resin bead #1), and variations by a factor of 3.0, 1.8, and 1.4 were observed along the inferior direction (caused by resin bead #4), respectively. Since the intrasource shielding effects were virtually constant along the source long-axes, these results justify the conclusion that anisotropy variations were largely dependent on geometric effects.

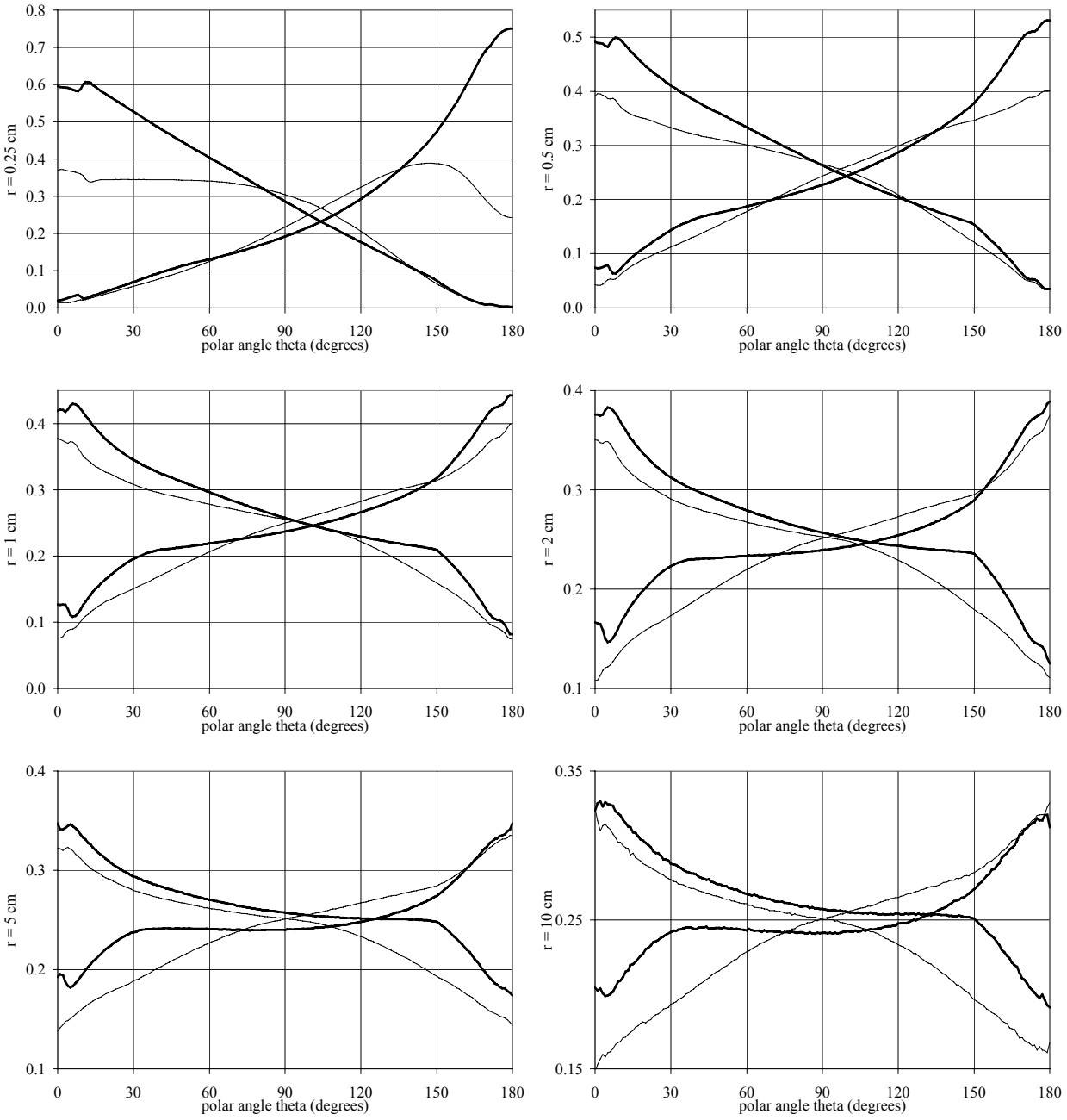

Figure 5. Contributions to the 2-D anisotropy function from each of the four resin beads. Fig. 5a through Fig. 5f depict the contributions from each resin bead at r = 0.25, 0.5, 1, 2, 5, and 10 cm, respectively. Note that the ordinate scale range diminishes as r increases. It is evident that the contributions significantly differ as the distance above or below the transverse-plane increases, and as radial distance diminishes.

3.3. Validation of Methodology

Results of the validation study are presented in Fig. 6 in comparison to results obtained when simply adding the resin bead #1 and #3 results. Fig. 6b shows the ratio of the validation results divided by the equally-weighted sum of the resin bead #1 and #3 results. Due to the smaller integration volume, statistical errors increased as θ approached either 0º or 180º. Also, statistical errors increased as radial distance increased due to ^{125}I attenuation. However, these errors were typically < 0.04% for $r \leq 2$ cm and 10º < θ < 170º. Clearly, any differences observed were not statistically significant, and differences less than 2% are not clinically relevant [18]. Based on the notation described in Section 2.2 and evidence from Fig. 6 below, one can safely conclude that: (1)+(3) = (1+3), and therefore that: (1)+(2)+(3)+(4) = (1+2+3+4). Consequently, the superposition-method was validated and upheld.

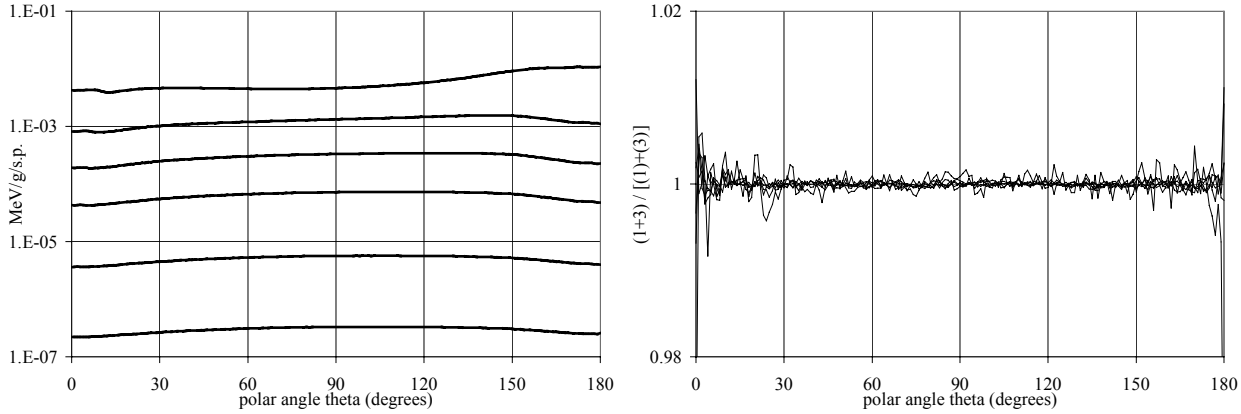

Figure 6. Fig. 6a illustrates raw MCNP output for the validation study (resin beads #1 + #3). Starting from the top, the curves are the 0.25, 0.5, 1, 2, 5, and 10 cm data. Fig. 6b illustrates these results normalized to the transverse-plane values (2-D anisotropy functions), and divided by the equally-weighted combination of resin bead #1 and resin bead #3 results. As expected, differences were negligible and not statistically significant.

4. CONCLUSIONS

Using Monte Carlo methods, the individual contributions from four resin beads were determined for a typical ^{125}I brachytherapy source using a superposition-methodology which was validated using a quasi-realistic source model. For distances beyond 0.5 cm on the transverse-plane, contributions to dose from each bead was relatively uniform. For $r \leq 0.5$ cm, contributions from resin bead #2 dominated while contributions from resin beads #3 and #4 became minimal. Off the transverse-plane, 2-D anisotropy function contributions were assessed. At small distances (e.g., r = 0.25 cm, the combined 2-D anisotropy function was largely dominated by contributions from resin beads #1 and #4 in the superior (θ = 0º) and inferior (θ = 180º) directions,

respectively. As distances increased, contributions among the four beads became more consistent with resin beads #1 and #2 and resin beads #3 and #4 comprising the major contributions in the superior and inferior directions, respectively. These results imply that significant variations in intrasource uniformity of ^{125}I activities would cause negligible variations on the transverse-plane at large distances. However, substantial variability in dose rate distributions would be exhibited at points close to the source and especially at points near the source long-axes.

REFERENCES

1. J. F. Williamson and A. S. Meigooni, "Quantitative dosimetry methods in brachytherapy," in: *Brachytherapy Physics* eds. J. F. Williamson, B. R. Thomadsen, and R. Nath (Medical Physics Publishing, Madison, WI, 1995) pp. 87-133.
2. J. F. Williamson, B. M. Coursey, L. A. DeWerd, W. F. Hanson, and R. Nath, "Dosimetric prerequisites for routine clinical use of new low energy photon interstitial brachytherapy sources," *Medical Physics*, **25**, pp.2269-2270 (1998)
3. R. Nath, M. J. Rivard, B. M. Coursey, L. A. DeWerd, W. F. Hanson, M. S. Huq, and J. F. Williamson, "Status of the American Association of Physicist in Medicine Radiation Therapy Committee Subcommittee's Low-Energy Interstitial Brachytherapy Source Dosimetry: Procedure for the development of consensus single source dose distributions," *Medical Physics*, **29**, pp.1349 (2002)
4. R. Nath, L. L. Anderson, G. Luxton, K. A. Weaver, J. F. Williamson, and A. S. Meigooni, "Dosimetry of interstitial brachytherapy sources: Recommendations of the AAPM Radiation Therapy Committee Task Group No. 43," *Medical Physics*, **22**, pp.209-234 (1995).
5. J. G. Wierzbicki, M. J. Rivard, D. S. Waid, and V. E. Arterbery, "Calculated dosimetric parameters of the IoGold ^{125}I source Model 3631-A," *Medical Physics*, **25**, pp.2197-2199 (1998).
6. J. G. Wierzbicki, D. S. Waid, M. J. Rivard, and V. E. Arterbery, "Radiographic characterization and energy spectrum of the IoGold ^{125}I source model 3631-A/S," *Medical Physics*, **26**, pp.392-394 (1999).
7. M. J. Rivard, "Monte Carlo calculations of AAPM Task Group Report No. 43 dosimetry parameters for the MED3631-A/M ^{125}I source," *Medical Physics*, **28**, pp.629-637 (2001).
8. M. J. Rivard, "A discretized approach to determining TG-43 brachytherapy dosimetry parameters: Case study using Monte Carlo calculations for the MED3633 ^{103}Pd source," *Applied & Radiation Isotopes*, **55**, pp.775-782 (2001).
9. M. J. Rivard, "Comprehensive Monte Carlo calculations of AAPM Task Group Report No. 43 dosimetry parameters for the Model 3500 I-Plant ^{125}I brachytherapy source," *Applied Radiation & Isotopes*, **57**, pp.381-389 (2002).
10. M. J. Rivard, "Comprehensive Monte Carlo calculations of AAPM Task Group No. 43 dosimetry parameters for the ^{125}I RL/RH, ^{103}Pd RL/RH, and ^{103}Pd SL/SH brachytherapy sources using conventional and modified MCNP cross-section libraries," *Medical Physics*, **30**, (in press) (2003).
11. "Computational Pile: Nuclear Sciences and Technology Division Linux Cluster," http://cpile.ornl.gov/ (2002).
12. J. F. Briesmeister. MCNP- A General Monte Carlo N-Particle Transport Code System, Version 4C, LA-13709-M (April, 2002)

13. J. J. DeMarco, R. E. Wallace, and K. Boedeker, "An analysis of MCNP cross-sections and tally methods for low-energy photon emitters," *Physics in Medicine & Biology*, **47**, pp.1321-1332 (2002).
14. "Bibliography of Photon Total Cross Section (Attenuation Coefficient) Measurements (online version 2.2)," http://physics.nist.gov/PhysRefData/photoncs/html/attencoef.html National Institute of Standards and Technology, Gaithersburg, MD (1998).
15. M. J. Rivard, J. G. Wierzbicki, F. Van den Heuvel, R. C. Martin, and R. R. McMahon, "Clinical brachytherapy with neutron emitting ^{252}Cf sources and adherence to AAPM TG-43 dosimetry protocol," *Medical Physics*, **26**, pp.87-96 (1999).
16. M. J. Rivard, "Dosimetry for ^{252}Cf neutron emitting brachytherapy sources: Protocol, measurements, and calculations," *Medical Physics*, **26**, pp.1503-1514 (1999).
17. M. J. Rivard, B. M. Coursey, L. A. DeWerd, W. F. Hanson, M. S. Huq, R. Nath, and J. F. Williamson, "Comment on: Let's abandon geometry factors other than that of a point source in brachytherapy dosimetry," *Medical Physics*, **29**, pp.1919-1920 (2002).
18. R. Nath, L. L. Anderson, J. A. Meli, A. J. Olch, J. A. Stitt, and J. F. Williamson, "Code of practice for brachytherapy physics: Report of the AAPM Radiation Therapy Committee Task Group No. 56," *Medical Physics*, **24**, pp.1557-1598 (1997).